Cell

Neuregulin1/ErbB4 Signaling Induces Cardiomyocyte Proliferation and Repair of Heart Injury

Kevin Bersell,[1] Shima Arab,[1] Bernhard Haring,[1,2] and Bernhard Kühn[1,2,*]
[1]Department of Cardiology, Children's Hospital, Boston, MA 02115, USA
[2]Department of Pediatrics, Harvard Medical School, Boston, MA 02115, USA
*Correspondence: bkuhn@enders.tch.harvard.edu
DOI 10.1016/j.cell.2009.04.060

SUMMARY

Many organs rely on undifferentiated stem and progenitor cells for tissue regeneration. Whether differentiated cells themselves can contribute to cell replacement and tissue regeneration is a controversial question. Here, we show that differentiated heart muscle cells, cardiomyocytes, can be induced to proliferate and regenerate. We identify an underlying molecular mechanism for controlling this process that involves the growth factor neuregulin1 (NRG1) and its tyrosine kinase receptor, ErbB4. NRG1 induces mononucleated, but not binucleated, cardiomyocytes to divide. In vivo, genetic inactivation of ErbB4 reduces cardiomyocyte proliferation, whereas increasing ErbB4 expression enhances it. Injecting NRG1 in adult mice induces cardiomyocyte cell-cycle activity and promotes myocardial regeneration, leading to improved function after myocardial infarction. Undifferentiated progenitor cells did not contribute to NRG1-induced cardiomyocyte proliferation. Thus, increasing the activity of the NRG1/ErbB4 signaling pathway may provide a molecular strategy to promote myocardial regeneration.

INTRODUCTION

Specific organ functions rely on differentiated cells. How differentiated cells are replaced is a fundamental question in biology with important implications for regenerative medicine. Although progenitor cells are important for regeneration in many organs, differentiated cells may also contribute by reverting to a proliferative state. Examples of differentiated cells contributing to tissue renewal are insulin-producing β cells in the mouse pancreas (Dor et al., 2004), heart muscle cells in regenerating zebrafish hearts (Poss et al., 2002), tracheal cells in *Drosophila* larvae during metamorphosis (Guha et al., 2008; Weaver and Krasnow, 2008), and *Arabidopsis* root cells after amputation of the stem cell niche (Sena et al., 2009).

If heart muscle cells, cardiomyocytes, can be induced to proliferate, it might be possible to regenerate heart muscle after myocardial infarction. Cardiomyocytes proliferate during prenatal development (Pasumarthi and Field, 2002). Soon after birth, however, cardiomyocytes become binucleated and withdraw from the cell cycle, giving rise to the notion that adult cardiomyocytes are incapable of proliferating; that is, they are terminally differentiated (Pasumarthi and Field, 2002). Specifically, cardiomyocytes in the adult mammalian heart are thought to be incapable of performing cytokinesis, the ultimate step of the mitotic cell cycle (Ahuja et al., 2007; Pasumarthi and Field, 2002).

Recent results challenge the paradigm that the adult heart is exclusively a terminally differentiated organ (Bergmann et al., 2009). Although cardiac regeneration has been studied for more than a century, little progress has been made in characterizing the mechanisms that control cell-cycle reentry of differentiated cardiomyocytes. Rather than attempt to answer the question about whether adult progenitor cells can give rise to new cardiomyocytes, we tested an alternative possibility—that cardiomyocytes have proliferative potential. We hypothesized that some differentiated cardiomyocytes are quiescent; that is, they do not proliferate under resting conditions but may proliferate in response to extracellular mitogens. To test this hypothesis, we used extracellular factors, such as fibroblast growth factor1 (FGF1), periostin, and neuregulin1 (NRG1), that activate receptors involved in cardiomyocyte proliferation during prenatal development (Pasumarthi and Field, 2002). NRG1 is an agonist for receptor tyrosine kinases of the epidermal growth factor receptor family, consisting of ErbB1, 2, 3, and 4 (Fuller et al., 2008). Binding of NRG1 to ErbB4 increases its kinase activity and leads to heterodimerization with ErbB2 or homodimerization with ErbB4 and stimulation of intracellular signal transduction pathways. Mice with germline knock-out of the *NRG1*, *ErbB2*, or *ErbB4* genes have thinner myocardium and die at midgestation, indicating that each of these genes is independently required for fetal cardiomyocyte generation (Gassmann et al., 1995; Lee et al., 1995; Meyer and Birchmeier, 1995).

The NRG1 receptor subunits ErbB2 and ErbB4 are also expressed in differentiated cardiomyocytes (Fuller et al., 2008). It became apparent that the NRG1/ErbB2/ErbB4 signaling complex is functionally active in differentiated cardiomyocytes when women receiving breast cancer treatment with the ErbB2-blocking antibody, Herceptin, developed cardiomyopathy (Keefe, 2002). In vitro studies have suggested that the

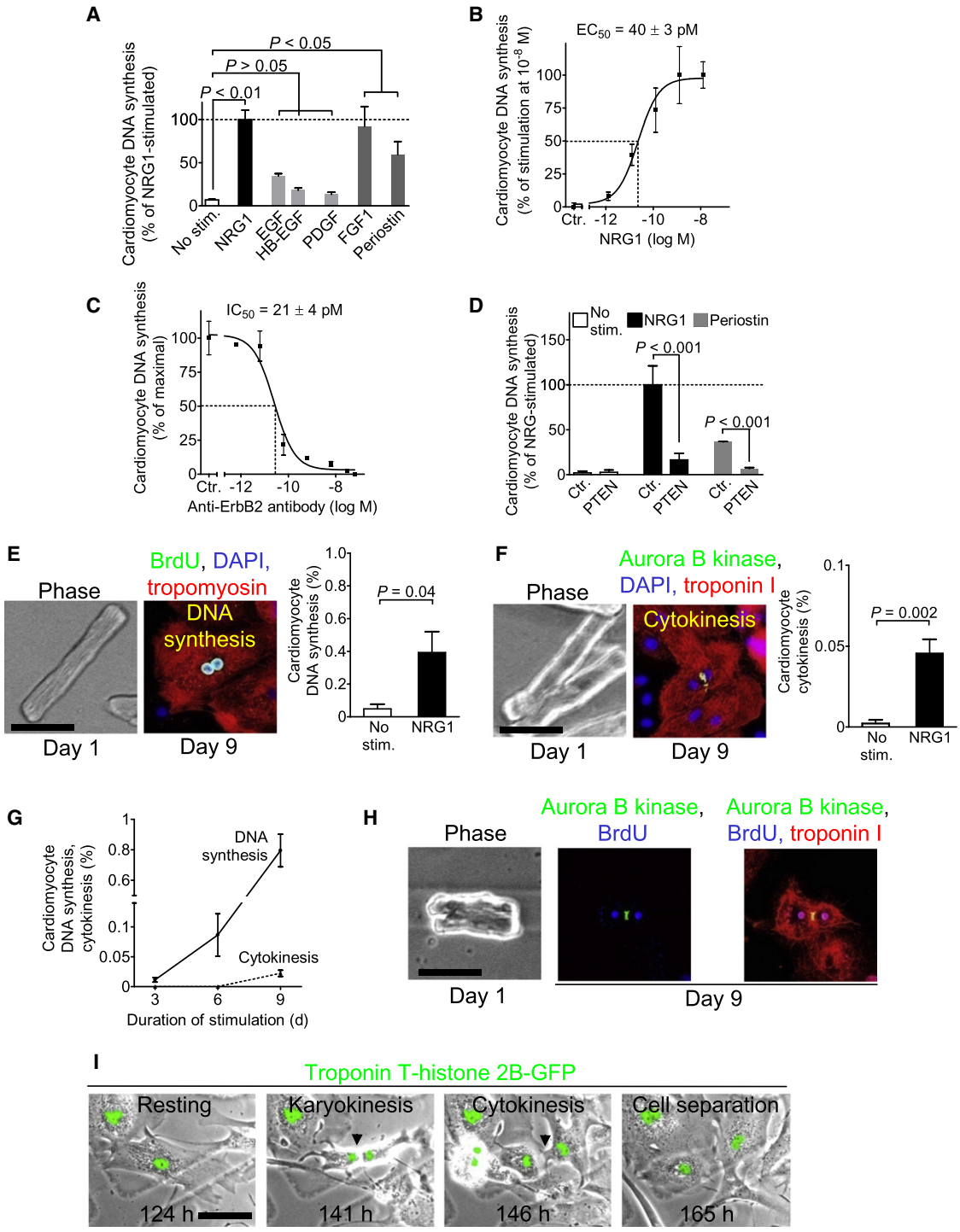

Figure 1. NRG1 Induces Cell-Cycle Reentry and Division of Differentiated Cardiomyocytes In Vitro

Primary adult rat ventricular cardiomyocytes were stimulated and labeled with BrdU for the last 3 days, and DNA synthesis was determined by immunofluorescence microscopy after 9 days.

(A) NRG1 (100 ng/ml), fibroblast growth factor 1 (FGF1, 100 ng/ml), and periostin (500 ng/ml) induce cardiomyocyte DNA synthesis, while epidermal growth factor (EGF), heparin-binding epidermal growth factor (HB-EGF), or platelet-derived growth factor BB (PDGF, 100 ng/ml each) do not. Results were normalized to NRG1 = 100%.

(B) NRG1-stimulated cardiomyocyte DNA synthesis was concentration dependent.

(C) NRG1-stimulated (125 pM) cardiomyocyte DNA synthesis inhibited with increasing concentrations of an antibody against ErbB2.

(D) Functional inhibition of PI3K with PTEN attenuates NRG1-stimulated DNA synthesis in cardiomyocytes.

NRG1/ErbB2/ErbB4 complex controls cardiomyocyte survival and myofibril disarray. However, these effects were not observed in knock-out mice in vivo (Fuller et al., 2008), indicating that ErbB2 and ErbB4 may act through other cellular mechanisms.

In this study, we show that NRG1 can induce mononucleated cardiomyocytes to proliferate. We reveal the underlying mechanisms and present a model of cardiomyocyte proliferation. Finally, we demonstrate that NRG1-induced cardiomyocyte proliferation promotes myocardial regeneration following myocardial injury.

RESULTS

NRG1 Stimulates Cell-Cycle Reentry and Division of Differentiated Cardiomyocytes

To identify factors that promote myocardial regeneration, we screened extracellular factors for their ability to induce DNA synthesis in primary adult rat ventricular cardiomyocytes. Three extracellular factors induced cardiomyocyte cell-cycle reentry. Two have been previously identified: fibroblast growth factor1 (FGF1; Engel et al., 2005) and periostin (Kuhn et al., 2007). The novel factor was the epidermal growth factor-like domain of NRG1β (Figure 1A; see also Figure S1 available online). NRG1 induced concentration-dependent DNA synthesis, which best fit a sigmoidal function, suggesting a receptor-mediated process (Figure 1B). The half-maximal stimulation EC_{50} was 40 ± 3 pM (n = 3; Figure 1B), indicating a high-affinity interaction with the receptor. In cardiomyocytes, NRG1 binds to ErbB4, which leads to formation and activation of ErbB2/ErbB4 hetero- or ErbB4/ErbB4 homodimers (Fuller et al., 2008). To determine whether ErbB2 is required for cardiomyocyte cell-cycle reentry, we added a fixed concentration of NRG1 (125 pM) and increasing concentrations of ErbB2-blocking antibody. The anti-ErbB2 antibody inhibited NRG1-stimulated DNA synthesis with an IC_{50} of 21 ± 4 pM (n = 3; Figure 1C), suggesting that ErbB2 is required for the NRG1 effect.

The phosphatidylinositol-3-OH kinase (PI3-kinase) pathway is required for cardiomyocyte cell-cycle reentry induced by FGF and periostin (Kuhn et al., 2007). Using functional inhibition with PTEN, we demonstrate that NRG1 also required the PI3-kinase pathway (Figure 1D), thus suggesting that different extracellular factors induce cardiomyocyte proliferation by activating pathways that converge at PI3-kinase. In summary, the ternary complex of NRG1, ErbB2, and ErbB4 enhances cardiomyocyte cell-cycle activity in a PI3-kinase-dependent mechanism.

To determine whether NRG1 induces differentiated cardiomyocytes to reenter the cell cycle, we ascertained the phenotype of individual cardiomyocytes before stimulation. NRG1 induced DNA synthesis in 0.4% ± 0.1% of cardiomyocytes over a period of 3 days (Figure 1E). We detected cytokinesis by visualizing aurora B kinase, a required component of the contractile ring at the site of cytoplasmic separation (Tatsuka et al., 1998). In NRG1-stimulated samples, 0.05% ± 0.01% of cardiomyocytes were in the process of cytokinesis (Figure 1F). Because most differentiated cardiomyocytes are multinucleated, it is possible that they undergo cytokinesis without prior DNA synthesis and karyokinesis. We therefore analyzed the time course of NRG1-induced cardiomyocyte DNA synthesis and cytokinesis and found that DNA synthesis preceded cytokinesis (Figure 1G). In addition, cardiomyocytes in cytokinesis had BrdU-positive nuclei, indicating that they underwent DNA synthesis prior to cytokinesis (Figure 1H).

To determine whether differentiated cardiomyocytes complete cytokinesis, we used video microscopy. NRG1 induced 3% ± 1.4% of differentiated cardiomyocytes to perform karyokinesis and 0.6% ± 0.3% to perform cytokinesis (n = 716). All of the observed cycling cardiomyocytes were viable for the entire duration of observation (75.4 ± 17.7 hr; range, 15–163 hr; n = 25). In summary, these data indicate that NRG1 induces differentiated cardiomyocytes to reenter the cell cycle from S phase and to complete cytokinesis in vitro.

Mononucleated Cardiomyocytes Have Proliferative Potential

Using video microscopy, we prospectively determined the proliferative potential of mono- and binucleated cardiomyocytes (Figure 1I; Movies S1 and S2). We found that NRG1 induced 32.6% ± 4.8% (n = 88) of mononucleated cardiomyocytes to perform karyokinesis. In contrast, only 1% ± 0.5% of all binucleated cardiomyocytes (n = 628) performed karyokinesis (p = 0.02, t test). Moreover, 45.8% ± 20.8% (n = 11) of mononucleated cardiomyocytes that entered cytokinesis also completed cytokinesis with abscission; the rest became binucleated. In total, 0.6% ± 0.3% of all cardiomyocytes divided, all of which were mononucleated.

ErbB4 Controls Postnatal Cardiomyocyte Proliferation In Vivo

To determine whether the NRG1/ErbB2/ErbB4 complex controls cardiomyocyte proliferation in postnatal hearts in vivo, we disrupted the complex by genetically inactivating the *ErbB4* gene. We treated α-*MHC-MerCreMer*$^{+/+}$; *ErbB4*$^{F/F}$ mice (test) and α-*MHC-MerCreMer*$^{+/+}$; *ErbB4*$^{Wt/F}$ mice (control littermates) with tamoxifen. Following ErbB4 inactivation on postnatal days 2–4, we analyzed the effect on postnatal day 19. Cardiomyocyte

(E and F) Optical fate mapping of individual cardiomyocytes. Representative examples of corresponding phase contrast images before stimulation and immunofluorescent images after 9 days of stimulation with NRG1 and labeling with BrdU for the final 3 days. Graphs show portion of cardiomyocytes performing DNA synthesis over a period of 3 days (E) and that were in cytokinesis on day 9 (F).

(G) Cardiomyocyte DNA synthesis precedes cytokinesis.

(H) BrdU-labeled cardiomyocyte in cytokinesis, indicating progression through the complete cell cycle.

(I) Mononucleated cardiomyocyte undergoing karyokinesis and cytokinesis. Histone 2B-GFP was expressed under control of the troponin T promoter (green) to visualize cardiomyocyte chromatin. Images were captured every 1 hr. Selected images are shown, as indicated at the bottom. The complete movie is provided in Movie S1. Arrowheads indicate cleavage furrow at 141 hr and 146 hr. Scale bars, 50 μm. No stim., no stimulation. Data are means ± standard error of the mean (SEM) from at least three experiments. Statistical significance was determined by ANOVA (A and D) and t test (E and F).

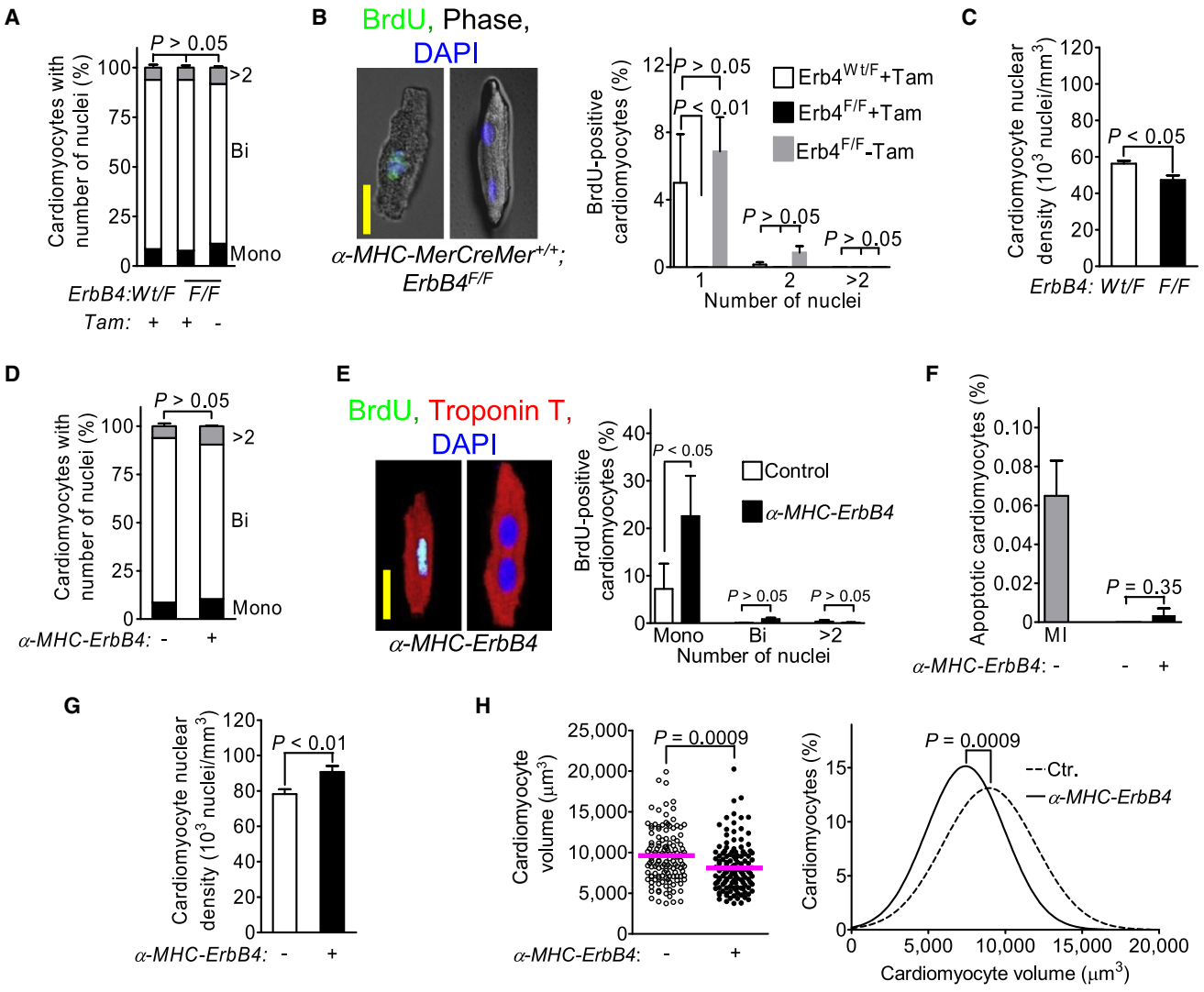

Figure 2. ErbB4 Controls Postnatal Cardiomyocyte Proliferation In Vivo

(A–C) Experiments were performed in *α-MHC-MerCreMer*$^{+/+}$*; ErbB4*$^{F/F}$ (test group) and in *α-MHC-MerCreMer*$^{+/+}$*; ErbB4*$^{Wt/F}$ (control group) mice. (A) Inactivation of *ErbB4* does not affect portion of mono- and multinucleated cardiomyocytes. (B and C) Inactivation of *ErbB4* abolishes postnatal cardiomyocyte cell-cycle activity (B) and disrupts cardiomyocyte proliferation (C).

(D–H) Experiments were performed in *α-MHC-ErbB4* mice (test group) and wild-type littermates (control group).

(D) Transgenic expression of *ErbB4* under control of the α-MHC promoter does not change the portion of mono- and multinucleated cardiomyocytes.

(E) Overexpressing *ErbB4* in differentiated cardiomyocytes increases cell-cycle activity of mononucleated cardiomyocytes. Examples of BrdU-positive mononucleated differentiated cardiomyocyte and BrdU-negative binucleated cardiomyocyte and quantification are shown.

(F) Overexpressing *ErbB4* has no effect on cardiomyocyte apoptosis. Positive control is 1 week after myocardial infarction, from Figure 7B.

(G and H) ErbB4-induced cardiomyocyte cell-cycle activity results in more (G) and smaller (H) cardiomyocytes. Scale bars 25 μm. Significance tested by ANOVA (A, B, and E) and t test (C, F–H). Results are means ± SEM from more than eight different hearts per experiment.

differentiation was not affected, as demonstrated by two observations: the formation of bi- and multinucleated cardiomyocytes was not altered (Figure 2A), and cardiomyocytes from test and control mice had indistinguishable morphology (Figure 2B). To determine whether ErbB4 is required for postnatal cardiomyocyte cell cycling, we quantified cardiomyocytes that incorporated BrdU (Figure 2B). After 5 injections of BrdU on postnatal days 16–18, test mice had no detectable cardiomyocyte BrdU uptake, whereas control mice had 5% ± 2.9% (n = 4) BrdU-positive mononucleated cardiomyocytes ($p < 0.01$, Figure 2B). Neither *α-MHC-MerCreMer*$^{+/+}$; *ErbB4*$^{F/F}$ mice in the absence of tamoxifen (Figure 2B) nor *α-MHC-MerCreMer*$^{+/+}$*;ErbB4*$^{Wt/Wt}$ mice treated with tamoxifen (Figure S2D) had reduced NRG1-induced cardiomyocyte cycling, thus confirming that inactivation of both ErbB4 alleles was required. To test whether the decrease in cell-cycle activity in ErbB4-inactivated mice would result in lower cardiomyocyte numbers, we determined the volume density of cardiomyocyte nuclei, which was 20% lower

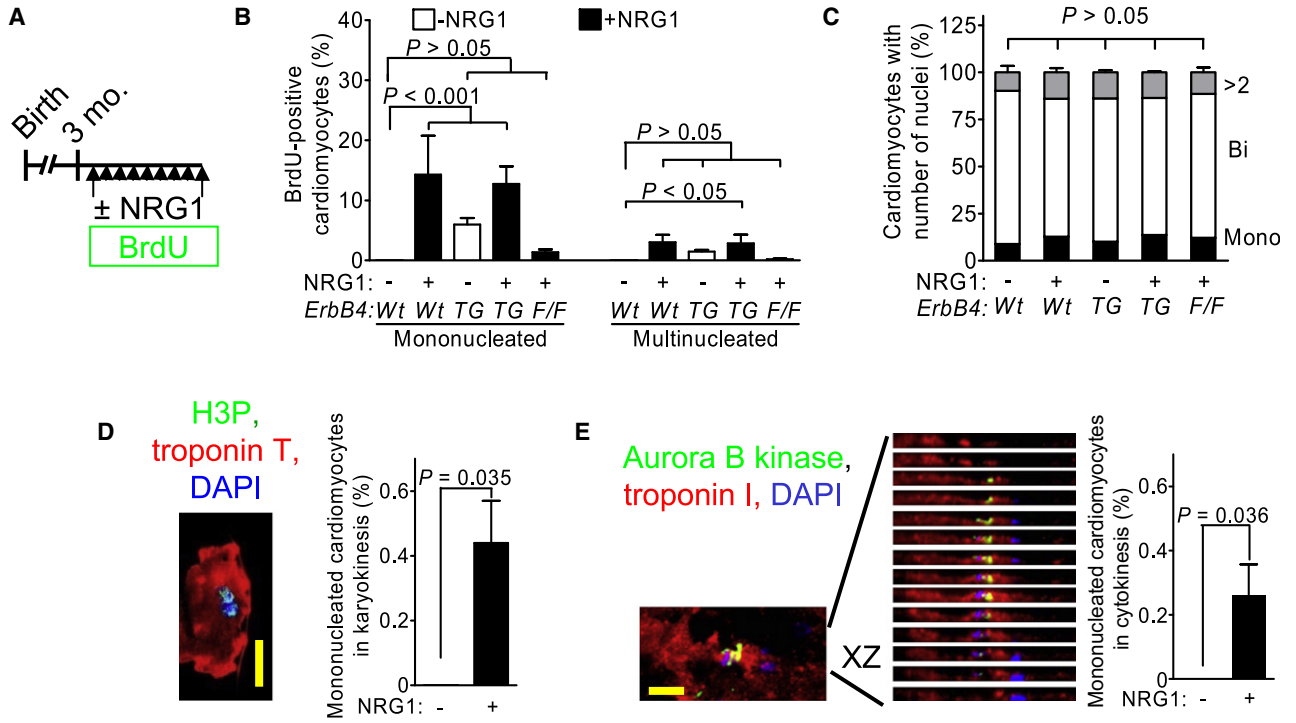

Figure 3. NRG1 Induces Cycling of Differentiated Cardiomyocytes In Vivo in an ErbB4-Dependent Mechanism

(A) Experimental design. Vertical arrowheads indicate daily NRG1 injections.

(B) ErbB4 controls NRG1-induced cardiomyocyte cell cycling.

(C) Proportions of mono-, bi-, and multinucleated cardiomyocytes are not affected by modulating NRG1/ErbB4 signaling.

(D and E) NRG1 induces cardiomyocyte karyokinesis (D) and cytokinesis (E). Aurora B-kinase-positive midbody is shown in a series of XZ reconstructions. Scale bar, 25 μm. Results are means ± SEM from at least five animals per experiment.

(Figure 2C; Table S1). Taken together, ErbB4 is required for normal postnatal cardiomyocyte proliferation.

To determine whether ErbB4 is sufficient to increase cycling of differentiated cardiomyocytes, we overexpressed ErbB4 under control of the α-MHC promoter (*α-MHC-ErbB4*; Tidcombe et al., 2003), which did not alter the percentage of mono- and multinucleated cardiomyocytes, indicating that ErbB4 did not affect the normal postnatal formation of multinucleated cardiomyocytes (Figure 2D). To analyze cardiomyocyte cell cycling, we quantified cardiomyocyte BrdU uptake. Control mice at 14 days of age had BrdU uptake in 7.2% ± 5.3% (n = 6) of mononucleated cardiomyocytes (Figure 2E). In contrast, *α-MHC-ErbB4* transgenic mice had BrdU uptake in 22.6% ± 8.5% (n = 5) of mononucleated cardiomyocytes, a 3-fold increase ($p < 0.05$). ErbB4-transgenesis did not affect cardiomyocyte apoptosis (Figure 2F). The increased cell-cycle activity in ErbB4-transgenic hearts resulted in a higher volume density of cardiomyocyte nuclei (Figure 2G), consistent with smaller cardiomyocytes (Figure 2H) of normal proportions (Figure S3). In the presence of identical myocardial mass and volume and identical proportions of mono- and multinucleated cardiomyocytes (Tables S2–S4; Figure 2D), this indicates that *α-MHC-ErbB4* transgenic hearts have more cardiomyocytes that are smaller. In summary, these results demonstrate that ErbB4 is sufficient to increase cardiomyocyte proliferation in vivo.

NRG1 Induces Cardiomyocyte Cell-Cycle Reentry, Karyokinesis, and Cytokinesis In Vivo

Cardiomyocytes in adult mammalian hearts do not proliferate under baseline conditions (Pasumarthi and Field, 2002). To determine whether stimulating the NRG1/ErbB4 signaling pathway induces cardiomyocyte cell-cycle reentry in vivo, we injected recombinant NRG1 in 3-month-old mice, labeled with BrdU in the drinking water for 9 days, and then quantified cardiomyocyte cell-cycle activity (Figure 3A). In control mice, we did not detect cycling cardiomyocytes (Figure 3B), in accordance with published results (Soonpaa and Field, 1998). In contrast, in mice injected with recombinant NRG1, 14.3% ± 6.5% of mononucleated and 3% ± 1.2% of multinucleated cardiomyocytes were BrdU positive ($n = 3$; $p < 0.001$; Figure 3B). Thus, NRG1 induces differentiated cardiomyocytes to leave proliferative quiescence.

We next determined whether the NRG1-induced cardiomyocyte cell-cycle reentry was mediated by ErbB4. Injecting NRG1 into *ErbB4*-transgenes did not increase cardiomyocyte cycling above the level of injecting NRG1 into littermate controls, suggesting that ErbB4 expression levels were not limiting cardiomyocyte cell-cycle reentry (Figure 3B). We then inactivated *ErbB4*, which resulted in a marked decrease of NRG1-induced cardiomyocyte DNA synthesis, indicating that ErbB4 was required for NRG1-induced cardiomyocyte cell-cycle reentry (Figure 3B). Importantly, the proportions of mono- and

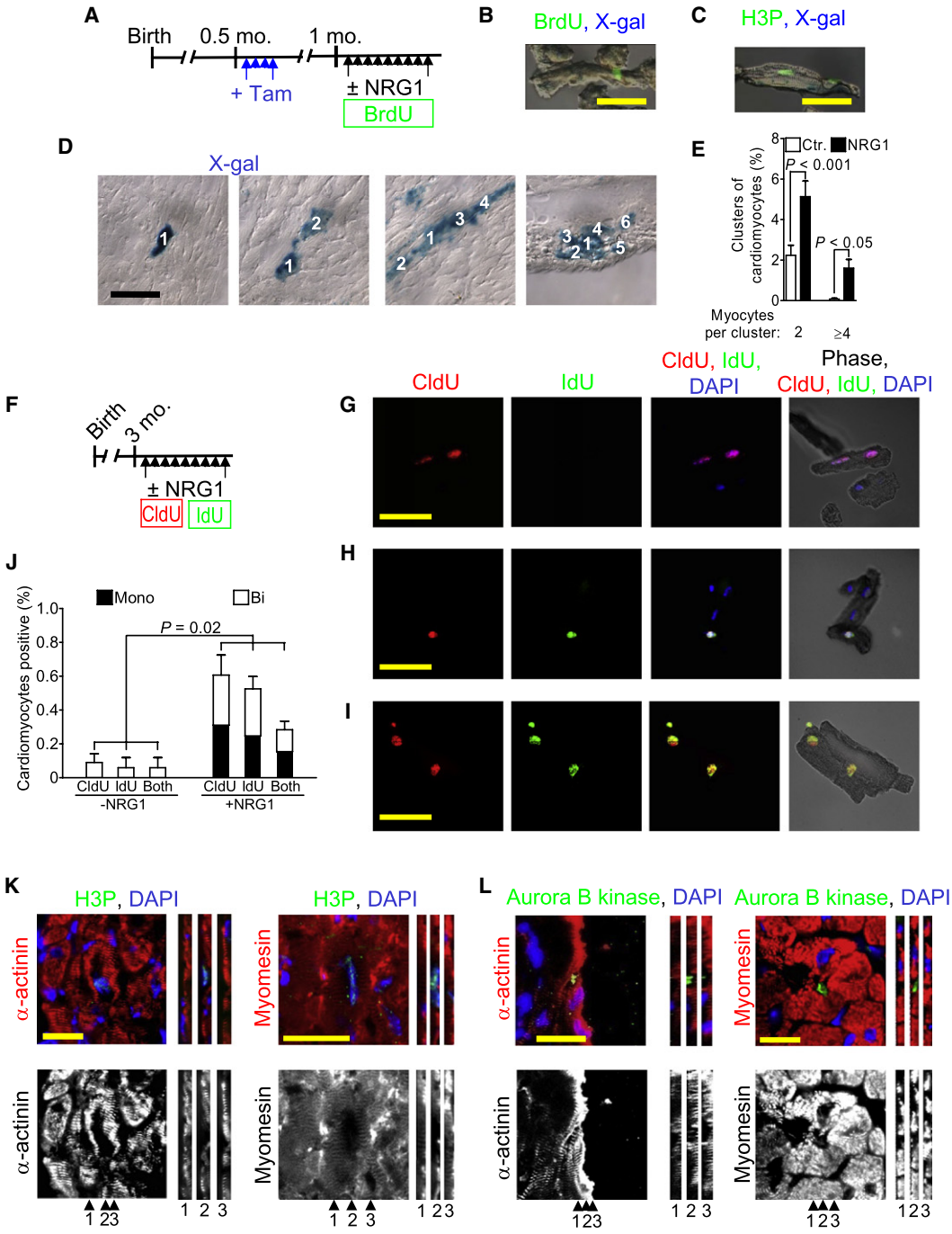

Figure 4. NRG1 Induces Proliferation of Differentiated Cardiomyocytes In Vivo

(A) Experimental design for genetic fate map using α-*MHC-MerCreMer*$^{+/+}$; *Rosa26R mice*$^{+/-}$. Vertical arrowheads indicate injections of tamoxifen (Tam) to induce permanent genetic labeling and NRG1 injections.

(B and C) NRG1-induced DNA synthesis (B) and karyokinesis (C) originate from differentiated cardiomyocytes, evident by X-gal staining.

(D and E) Representative examples of cardiomyocyte clusters after 9 NRG1 injections (D) and quantification (E).

(F) Cardiomyocyte proliferation in adult mice (3 months) was induced with 9 daily injections of NRG1. Repeated transition through the S phase of the cell cycle was detected by successively labeling with the thymidine analogs chlorodeoxyuridine (CldU) and iododeoxyridine (IdU).

(G) Example of a binucleated cardiomyocyte after one S phase transition.

(H and I) Examples of mononucleated (H) and binucleated (I) cardiomyocytes after two rounds of S phase transition. An isolated nucleus is attached to the outside of the cardiomyocyte in (I).

(J) Diagram of portion of cardiomyocytes by frequency of cell-cycle transitions and number of nuclei.

multinucleated cardiomyocytes were not different between the experimental groups (Figure 3C). We determined whether NRG1 induced cardiomyocyte karyokinesis (Figure 3D). In NRG1-injected animals, 0.4% ± 0.1% of mononucleated cardiomyocytes were in the process of karyokinesis, but none in controls. We then quantified cardiomyocyte cytokinesis, the terminal phase of the cell cycle (Figure 3E). In NRG1-injected animals, 0.3% ± 0.1% of mononucleated cardiomyocytes were in the process of cytokinesis, but none in control animals. In summary, activating NRG1/ErbB4 signaling induces quiescent cardiomyocytes to reenter the cell cycle and to undergo karyokinesis and cytokinesis in vivo.

NRG1-Induced Cell-Cycle Activity In Vivo Stems from Differentiated Cardiomyocytes

What is the cellular source of NRG1-induced cardiomyocyte cell-cycle activity? The in vitro optical fate mapping suggested that NRG1 induces differentiated cardiomyocytes to reenter the cell cycle. To test this possibility in vivo, we performed a genetic fate map. Using α-*MHC-MerCreMer*; *Rosa26R* mice, we permanently labeled differentiated cardiomyocytes (Figures 4A and S2C). We then injected NRG1 and quantified BrdU uptake. We did not detect BrdU-positive cardiomyocytes in the control group. In NRG1-treated animals, in contrast, we identified BrdU-positive cardiomyocytes that were X-gal positive, indicating that they were differentiated before they reentered the cell cycle (Figure 4B). We also found X-gal-positive cardiomyocytes during karyokinesis (Figure 4C). In conclusion, NRG1 induces differentiated cardiomyocytes to reenter the cell cycle.

NRG1 Induces Proliferation of Differentiated Cardiomyocytes In Vivo

Whether differentiated cardiomyocytes can proliferate is a controversial question in cardiovascular biology. To answer this question in vivo, we analyzed the fate of genetically labeled differentiated cardiomyocytes. We induced sparse genetic labeling of differentiated cardiomyocytes in α-*MHC-MerCreMer*$^{+/+}$; *Rosa26R*$^{+/-}$ mice (Figure S4). One week later, we induced cardiomyocyte proliferation by injecting NRG1 for nine days and quantified the number of multicellular X-gal-positive clusters of cardiomyocytes. The majority of X-gal-positive cardiomyocytes were single (Figures 4D and S4). NRG1-injected animals (n = 9) had 2.1-fold more clusters of two and 35-fold more clusters consisting of four and more cardiomyocytes than did control animals (n = 10; Figure 4E). In conclusion, NRG1 induces proliferation of differentiated cardiomyocytes in vivo.

To determine whether cardiomyocytes can undergo successive cell divisions in vivo, we labeled with chlorodeoxyuridine (CldU) for the first 4 days, followed by a 1-day washout period, and then with iododeoxyuridine (IdU) for the final 4 days of NRG1 injections (Figure 4F). We readily identified cardiomyocytes that were labeled with one thymidine analog, indicating that they were in the cell cycle once (Figure 4G). We detected mononucleated cardiomyocytes that took up both thymidine analogs, signifying that they had gone through S phase, completed cytokinesis, and cycled again at least once more (Figure 4H). We also detected binucleated cardiomyocytes that took up both thymidine analogs (Figure 4I). Quantification of the frequency of cell-cycle transition in NRG1-stimulated hearts showed that 0.6% ± 0.2% of cardiomyocytes took up CldU during the first 4 days, and 0.5% ± 0.1% of cardiomyocytes took up IdU during the final 4 days of NRG1 stimulation (Figure 4J). Of note, 50% ± 0.08% of mononucleated cardiomyocytes that went through the cell cycle during the first 4 days of NRG1 stimulation underwent another round of replication during the final 4 days (Figure 4J). Of cardiomyocytes that were double labeled (i.e., that had transitioned two cell cycles), 58% ± 5.9% (n = 117) were mononucleated, indicating that they completed cytokinesis, consistent with our video microscopy data. Because the presence of both thymidine analogs in a mononucleated cardiomyocyte allowed us to conclude that they underwent cytokinesis at least once, we can determine the frequency of cytokinesis, which was 0.15% ± 0.04% of all cardiomyocytes over a period of 4 days in NRG1-injected animals, but zero in control animals. In conclusion, NRG1 stimulates a significant portion of mononucleated cardiomyocytes to replicate.

Cytokinesis is a particular challenge for differentiated cardiomyocytes because they contain contractile fibrils organized in sarcomeres. This raises an important question: how do differentiated cardiomyocytes divide their nuclei and cell bodies? To address this question, we visualized the sarcomeric structure in dividing cardiomyocytes. During karyokinesis, the sarcomeric Z-disks and M-bands were disassembled in the region of the midzone (Figure 4K). Notably, in cytokinesis, the sarcomeric structure was absent from the division plane (Figure 4L). In conclusion, cardiomyocyte division is associated with sarcomere disassembly.

Undifferentiated Progenitor Cells Do Not Contribute to NRG1-Induced Cardiomyocyte Proliferation

Our results thus far indicate that NRG1 induces differentiated cardiomyocytes to proliferate. However, generation of cardiomyocytes from undifferentiated progenitor cells may also contribute to the observed effect. If NRG1-induced cardiomyocyte proliferation had two different cellular origins—that is, stemmed from differentiated cardiomyocytes and from undifferentiated progenitor cells—then there should be detectable differences between both processes. We labeled differentiated cardiomyocytes genetically by activating the α-*MHC-MerCreMer*$^{+/+}$; *Rosa26R*$^{+/+}$ system. A hallmark of cardiomyocytes derived from undifferentiated stem or progenitor cells is that they do not carry

(K) Cardiomyocytes in karyokinesis, visualized with an antibody against phosphorylated histone 3B (H3B) begin to disassemble their contractile apparati, visualized with a Z-disk marker (α-actinin) and an M-band marker (myomesin).

(L) Cardiomyocytes in cytokinesis, visualized with an antibody against aurora B kinase, have complete disassembly of the contractile apparatus, visualized with antibodies against a Z-disk marker (α-actinin) and an M-band marker (myomesin). Perpendicular reconstructions are indicated with numbered arrowheads. Color codes are indicated at the top. Statistical significance was determined by ANOVA (E and J). Scale bars 25 μm (B, C, K, and L) and 100 μm (D and G–I). Results are means ± SEM of at least seven animals per experiment.

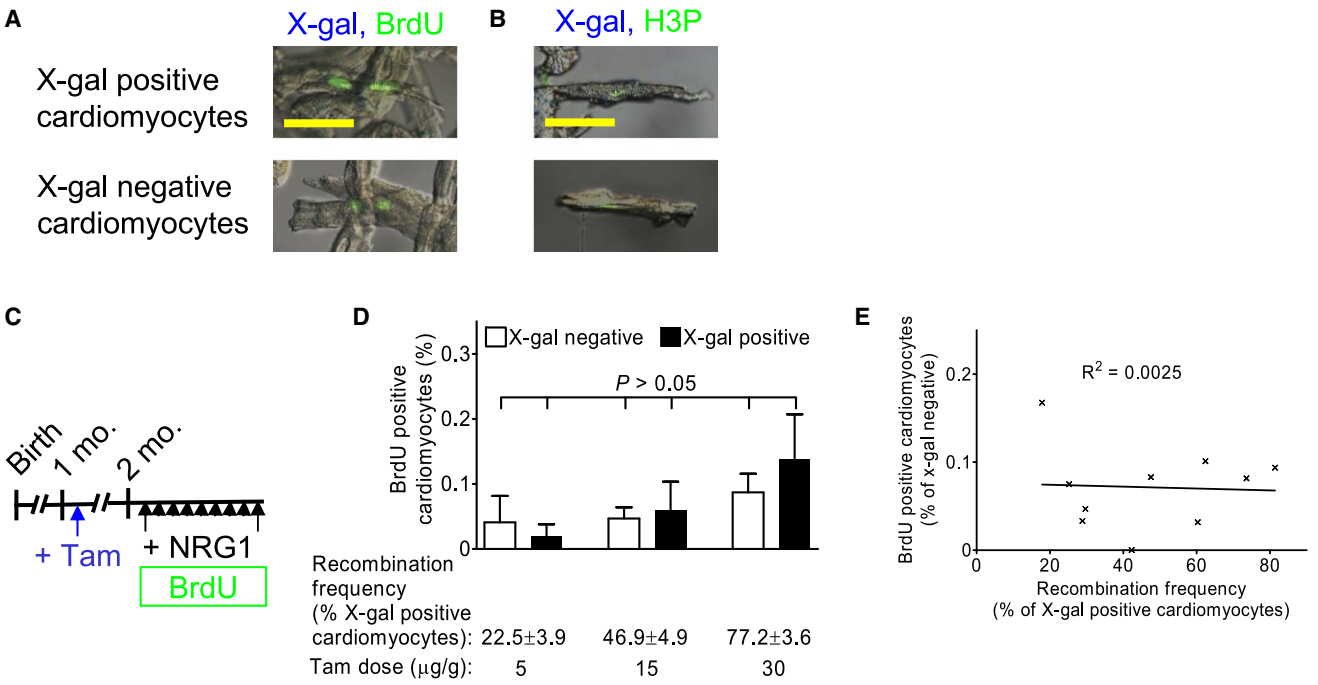

Figure 5. Undifferentiated Progenitor Cells Do Not Contribute to NRG1-Induced Cardiomyocyte Cell-Cycle Activity

(A and B) Examples of X-gal-positive and -negative differentiated cardiomyocytes that had undergone DNA synthesis (A) and mononucleated cardiomyocyte in the cell cycle (B), which have identical morphology, suggesting similar cellular origins.

(C) Experimental design for dynamic genetic fate map. Differentiated cardiomyocytes were genetically labeled by activation of β-galactosidase transcription, visualized by X-gal staining. Cardiomyocyte proliferation was induced by injecting NRG1 into adult mice (2 months of age).

(D) Stepwise incremental genetic labeling demonstrates lack of correlation between genetic labeling frequency and NRG1-induced cardiomyocyte generation, thus indicating that genetically labeled and unlabeled cardiomyocytes originate from differentiated cardiomyocytes.

(E) Regression of NRG1-induced cardiomyocyte generation and recombination frequency shows lack of correlation between genetic labeling frequency and cell-cycle activity in the genetically unlabeled fraction, indicating that NRG1-induced cardiomyocyte proliferation originates from differentiated cardiomyocytes. Color codes indicated at the top. Scale bars 50 μm. Statistical significance was determined by ANOVA (D) and by linear regression (E). Results are means ± SEM from more than 11 animals per experiment.

the α-MHC promoter-dependent genetic label (Hsieh et al., 2007). Thus, genetically labeled cardiomyocytes are derived from differentiated cardiomyocytes. In contrast, cardiomyocytes without the genetic label could be derived from differentiated cardiomyocytes or from undifferentiated progenitor cells. After applying the genetic label, we induced proliferation with NRG1 and labeled with BrdU to visualize newly generated cardiomyocytes. To determine the contribution of progenitor cells to NRG1-induced cardiomyocyte proliferation, we compared BrdU-positive, X-gal-positive (cardiomyocyte-derived) with BrdU-positive, X-gal-negative cardiomyocytes (possibly progenitor cell-derived). The morphology of newly generated X-gal-positive and X-gal-negative cardiomyocytes was identical (Figure 5A). We visualized cardiomyocytes that were presently in the cell cycle with H3P staining and compared X-gal-positive with X-gal-negative cardiomyocytes, which were identical (Figure 5B). These results suggested that X-gal-positive and X-gal-negative BrdU-positive cardiomyocytes had the same cellular origin (i.e., they originated from differentiated cardiomyocytes).

Because differentiated cardiomyocytes and undifferentiated progenitor cells may have different proliferative rates, we compared the proportion of BrdU-positive cardiomyocytes derived from either origin. Cardiomyocytes stemming from differentiated cardiomyocytes are BrdU positive and X-gal positive, and cardiomyocytes stemming from undifferentiated progenitor cells are BrdU positive and X-gal negative. We compared the percentage of BrdU-positive cardiomyocytes across a range of genetic labeling frequencies (Figures 5C and 5D). We found that the proliferative rates were identical in X-gal-negative and X-gal-positive cardiomyocytes at low, intermediate, and high genetic labeling frequencies, indicating that NRG1-induced cardiomyocyte proliferation stemmed from a single cellular source (Figure 5D).

If there was an influx of cardiomyocytes from undifferentiated progenitor cells, then the measured proliferative rate in this portion should increase with increasing fraction of X-gal-positive cardiomyocytes. Thus, we correlated the proliferative rate of X-gal-negative cardiomyocytes with the genetic labeling frequency (Figure 5E). We found no correlation between the proliferative rate of X-gal-negative cardiomyocytes and the X-gal labeling frequency, thus excluding the influx of cardiomyocytes from undifferentiated progenitor cells. In summary, NRG1-induced cardiomyocyte proliferation has a single source, which stems from differentiated cardiomyocytes.

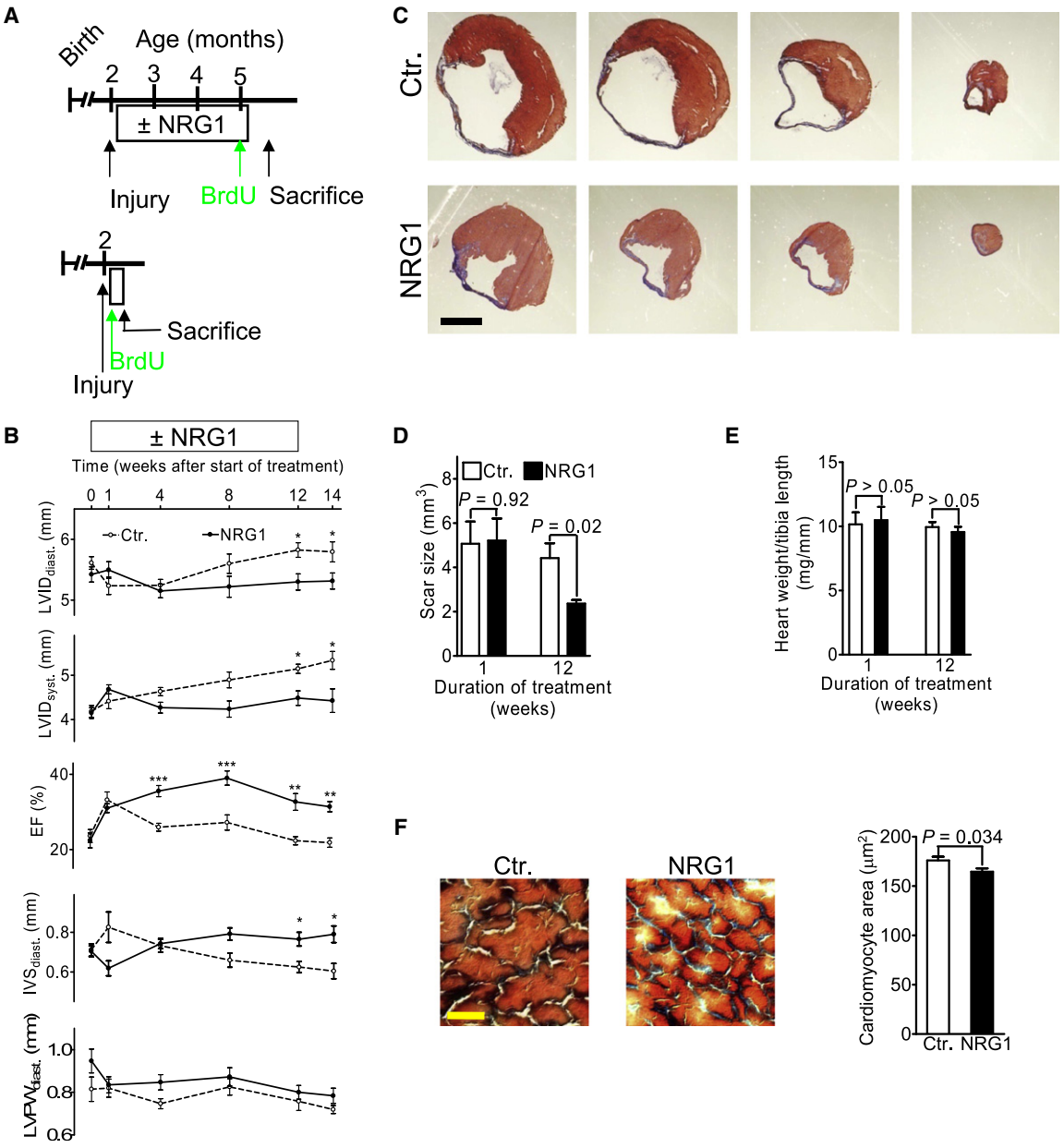

Figure 6. NRG1 Treatment Improves Myocardial Function and Induces Scar Regression

(A) Experimental design. Myocardial infarction was induced at 2 months of age. NRG1 or vehicle injections were begun 1 week later and continued for 1 or for 12 weeks. All mice were treated with BrdU in the drinking water during the final week of injections as indicated by the green arrow. Animals in the 12-week treatment arm were euthanized 2 weeks later to determine whether NRG1 effects were permanent.

(B) NRG1 treatment improves ventricular remodeling and myocardial function as shown by echocardiographic measurements of left ventricular internal dimensions (LVID), interventricular septum (IVS), left ventricular posterior wall (LVPW), and ejection fraction (EF).

(C and D) Infarct scar of representative examples of control and NRG1-treated hearts (C) and quantification (D).

(E) Heart weight is not affected by NRG1 treatment.

(F) Cardiomyocyte cross-sectional area is lower in NRG1-treated hearts. Statistical significance determined by ANOVA (B, D, and E) and t test (F). Scale bars 2 mm (C) and 50 μm (F). Results are means ± SEM from 10–32 animals.

NRG1 Improves Cardiac Function and Structure after Myocardial Infarction

To determine whether inducing cardiomyocyte proliferation with NRG1 is beneficial after myocardial injury, we permanently ligated the left anterior descending coronary artery (LAD) in 2-month-old mice and began daily NRG1 injections one week later for 12 weeks. Because regeneration would be anticipated to produce a permanent structural change, we introduced a

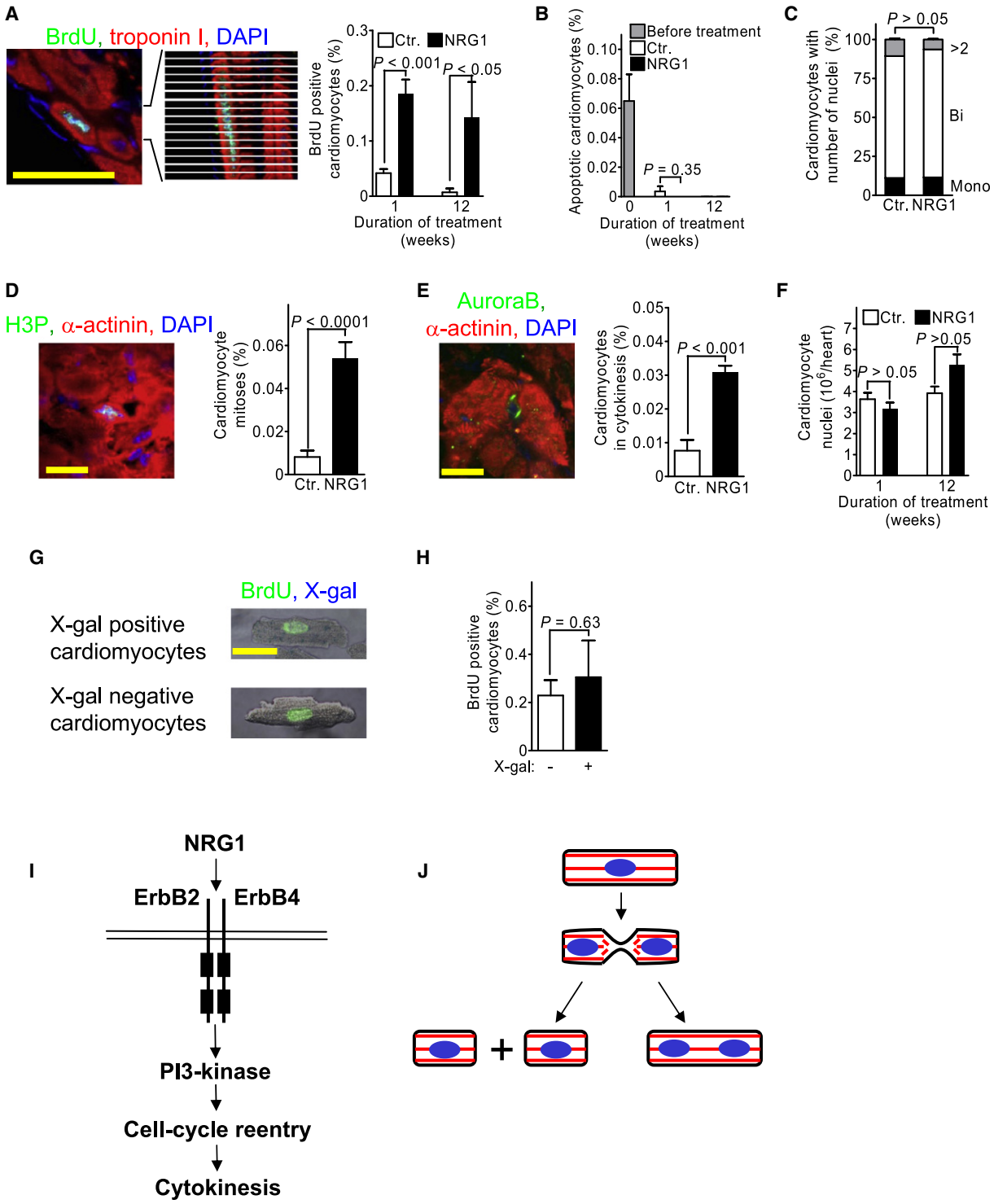

Figure 7. NRG1 Promotes Cardiomyocyte Proliferation after Myocardial Infarction

(A) Quantification of cardiomyocyte DNA synthesis after 1 week of continuous labeling with BrdU. Representative BrdU-positive cardiomyocyte in scar region.

(B) NRG1 treatment does not affect cardiomyocyte apoptosis.

(C) NRG1 treatment does not affect percentage of mono- and multinucleated cardiomyocytes.

(D) Quantification of cardiomyocyte mitoses by visualization of metaphase chromosomes. H3P-positive cardiomyocyte in scar region.

(E) Quantification of cardiomyocyte cytokineses by visualization of the contractile ring.

(F) Quantification of left ventricular cardiomyocyte nuclei shows significant cardiomyocyte replacement after 12 weeks of NRG1 treatment.

2 week window of no injections before the end of the experiment (Figure 6A). We determined myocardial structure and function by serial echocardiography (Figure 6B; Table S5). Over the course of the 15-week experiment, NRG1-injected animals had no significant increase of the dimension of the left ventricle, whereas control animals had significant left ventricular dilatation, indicating a positive effect of NRG1 on postinfarction remodeling. Injecting NRG1 induced a sustained improvement of myocardial function, determined by ejection fraction. Compensatory hypertrophy, determined by measuring the thickness of the interventricular septum and the left ventricular free wall, was significantly attenuated in NRG1-injected animals. In summary, NRG1 induced sustained improvements after myocardial infarction.

To analyze at the tissue level how NRG1 improved myocardial function, we determined the size of the infarct scar (Figure 6C, S5, and S6). After 1 week of treatment, control and NRG1-treated hearts had the same scar size; however, after 12 weeks of treatment and 2 additional weeks without treatment, NRG1-injected animals had a 46% smaller infarct scar (Figure 6D). We then compared the heart weight, which was identical at the beginning and 2 weeks after completion of treatment (Figure 6E). The cardiomyocyte cross-sectional area, however, was smaller in NRG1-treated hearts, consistent with attenuation of cardiomyocyte hypertrophy (Figure 6F). Collectively, these results indicate that administration of NRG1 for 12 weeks results in permanently improved myocardial function, smaller infarct scar size, and attenuated myocardial hypertrophy.

NRG1 Promotes Replacement of Cardiomyocytes after Myocardial Infarction

What are the underlying cellular mechanisms for the NRG1-induced improvements? To determine whether the decreased infarct scar size correlated with cardiomyocyte cell-cycle reentry, we quantified cardiomyocyte BrdU uptake. NRG1 increased cardiomyocyte BrdU uptake by 4.4-fold to 0.18% ± 0.03% without affecting cardiomyocyte apoptosis or changing the percentage of mono- and binucleated cardiomyocytes (Figures 7A–7C). Thus, NRG1 increased cardiomyocyte cell-cycle activity after myocardial infarction.

Can NRG1-induced cardiomyocyte cell-cycle activity account for the observed improvements? By visualizing cardiomyocytes in metaphase, we determined that 2,043 cardiomyocytes per heart were in karyokinesis (Figure 7D). In conjunction with the duration of karyokinesis of 1.8 ± 0.3 hr, determined by video microscopy (n = 18), this would result in 2.3×10^6 replaced cardiomyocyte nuclei over 12 weeks. We also quantified the portion of cardiomyocytes with a contractile ring (Figure 7E), which, in conjunction with a duration of cytokinesis of 1.6 ± 0.3 hr (n = 10), would result in 722,610 new cardiomyocytes in NRG1-injected animals over 12 weeks. We then quantified cardiomyocyte nuclei directly. NRG1-treated hearts had 1.4×10^6 more cardiomyocyte nuclei, equivalent to 690,000 more cardiomyocytes after 12 weeks (Figure 7F). Thus, NRG1-induced cardiomyocyte proliferation can account for the observed cardiomyocyte replacement.

To determine the cellular source of NRG1-induced cardiomyocyte replacement after injury, we permanently labeled differentiated cardiomyocytes with a genetic tag. We found that cycling cardiomyocytes that were genetically labeled were identical in morphology and proliferative rate to unlabeled cardiomyocytes (Figures 7G and 7H), indicating that undifferentiated stem and progenitor cells did not contribute to NRG1-induced cardiomyocyte replacement.

Bone marrow-derived c-kit-positive progenitor cells are required for the endogenous repair process after myocardial infarction (Fazel et al., 2006). The frequency of c-kit-positive cells was identical in control and in NRG1-injected animals (Figure S6), suggesting that NRG1 did not affect recruitment of c-kit-positive cells.

DISCUSSION

Our study demonstrates that differentiated cardiomyocytes can be induced to proliferate by activating NRG1/ErbB4 signaling, leading to enhanced myocardial regeneration and improved heart function. These findings offer a new strategy to promote the repair process after myocardial infarction. Several lines of evidence support this notion. First, we show that NRG1 induces differentiated cardiomyocytes to divide. Second, we show that NRG1-induced cardiomyocyte proliferation requires ErbB4. Third, we demonstrate that mononucleated differentiated cardiomyocytes disassemble their sarcomeres during division. Finally, we show that NRG1-induced cardiomyocyte proliferation promotes cardiac repair.

Molecular Mechanisms of Cardiomyocyte Proliferation

Stimulation of cell-cycle activity by extracellular NRG1 suggests that non-cell-autonomous mechanisms control the return of differentiated cardiomyocytes into a proliferative state. A similar mechanism operates in differentiated tracheal cells, which are induced to proliferate by FGF signaling during *Drosophila* metamorphosis (Guha et al., 2008; Weaver and Krasnow, 2008). Our NRG1/ErbB4 model is the latest addition to a number of molecular strategies used to augment mammalian heart regeneration: administration of recombinant periostin peptide (Kuhn et al., 2007) and FGF administration with inhibition of p38 mitogen-activated kinase (Engel et al., 2006; Engel et al., 2005). Interestingly, all four extracellular factors known to induce proliferation of differentiated cardiomyocytes (i.e., IGF1, FGF1, periostin, and NRG1) require PI3-kinase (Figure 7I). It is important to note that IGF1 and FGFs also induce cardiac hypertrophy, whereas NRG1 does not. In addition, cell-cycle activators (e.g., simian virus 40 large T antigen, cyclin A2, and cyclin D2) have been expressed in cardiomyocytes (Chaudhry et al., 2004; Katz et al., 1992; Pasumarthi et al., 2005), resulting in increased cardiomyocyte proliferation. Thus, very specific signals at the receptor, postreceptor, and at cell-cycle control levels may

(G and H) Examples (G) and quantification (H) of X-gal-positive and -negative differentiated mononucleated cardiomyocytes that had undergone DNA synthesis, which have identical morphology, suggesting similar cellular origins.
(I and J) Molecular (I) and cellular models (J) of cardiomyocyte proliferation. Results are means ± SEM from 11–24 animals.

induce differentiated cardiomyocytes to reenter the cell cycle. Periostin (Kuhn et al., 2007) and FGF1 (Engel et al., 2006) were locally administered, but we applied NRG1 systemically, thus increasing the translational potential.

Proliferating Cardiomyocytes Have Some Characteristics of Facultative Stem Cells

Facultative stem cells are in proliferative quiescence during adult life but return to a proliferative state upon stimulation (Rawlins and Hogan, 2006). It is formally possible that NRG1 can induce undifferentiated cardiac progenitor cells to proliferate and subsequently differentiate into mature cardiomyocytes (Chen et al., 2007; Hsieh et al., 2007). To exclude this as an explanation for our experimental results and to demonstrate that NRG1 induces proliferation of differentiated cardiomyocytes, we provide four lines of evidence: first, we showed with fate-mapping in vitro and in vivo that NRG1 induces differentiated cardiomyocytes to reenter the cell cycle. Second, we demonstrated that individual differentiated cardiomyocytes can give rise to multicellular clusters in vivo. Third, using dynamic genetic labeling in vivo, we demonstrated that NRG1-induced cardiomyocyte proliferation does not result from undifferentiated stem or progenitor cells. Fourth, NRG1 does not increase immigration of circulating c-kit-positive cells. Thus, our results indicate that NRG1 and ErbB4 control proliferation of a portion of differentiated cardiomyocytes.

Cellular Mechanisms of Cardiomyocyte Proliferation

We determined that, in vitro, NRG1 induces approximately 0.6% of all differentiated cardiomyocytes to divide over a period of 9 days. This finding is in agreement with approximately 0.15% of cardiomyocytes dividing over a 4-day period in vivo (Figure 4J) and 1.7% giving rise to multicellullar clusters over a 9-day period in vivo (Figure 4E). In comparison, in newts, lower vertebrates that regenerate their hearts, 29% of cardiomyocytes have proliferative capacity (Bettencourt-Dias et al., 2003). Zebrafish, which are also capable of cardiac regeneration, have more than 95% mononucleated cardiomyocytes with proliferative potential (Wills et al., 2008). Thus, the higher regenerative capacity of adult newt and zebrafish hearts may be related to the higher prevalence of proliferation-competent mononucleated cardiomyocytes in these species (Table S6).

We demonstrated that mononucleated cardiomyocytes have a higher proliferative potential than do binucleated cardiomyocytes. Mononucleated, but not binucleated, cardiomyocytes can complete cytokinesis. However, not all mononucleated cardiomyocytes that perform karyokinesis go on to divide. Approximately 50% of mononucleated cardiomyocytes that reentered the cell cycle also completed cyctokinesis. The other 50% did not and became binucleated (Figure 7J). Although the factors that control whether a mononucleated cardiomyocyte divides or becomes binucleated are unknown, this mechanism maintains the pool of proliferation-competent mononucleated cardiomyocytes, while generating terminally differentiated binucleated cardiomyocytes.

That differentiated cardiomyocytes may be capable of reentering the cell cycle has been repeatedly proposed throughout the past century (Pasumarthi and Field, 2002; Soonpaa and Field, 1998). However, it was suggested that the presence of differentiated sarcomeres is incompatible with cytokinesis (Ahuja et al., 2007). If cardiomyocytes can divide, they must possess mechanisms coordinating the cellular changes required for karyokinesis and cytokinesis with the presence of sarcomeres. We demonstrated here that differentiated cardiomyocytes disassemble their sarcomeres in the midzone during karyokinesis and cytokinesis. Thus, our data indicate that the presence of the differentiated cardiomyocyte contractile apparatus does not prohibit karyokinesis or cytokinesis.

It is tempting to propose that NRG1 induces permanent sarcomeric dedifferentiation in adult cardiomyocytes, which may facilitate their proliferation. We did not find evidence for general cardiomyocyte dedifferentiation in NRG1-injected or *ErbB4*-transgenic animals. Furthermore, NRG1 induces differentiation of embryonic stem cells into cardiomyocytes (Wang et al., 2008) and *NRG1*, *ErbB2*, and *ErbB4*-deficient mice lack myocardial trabeculations (Gassmann et al., 1995; Lee et al., 1995; Meyer and Birchmeier, 1995), suggesting that NRG1 and its receptors may control cardiomyocyte differentiation during development. We demonstrated here that NRG1 and ErbB4 regulate cardiomyocyte proliferation during postnatal life, consistent with pleiotropic effects of NRG1 that depend on the tissue context.

NRG1-Induced Cardiomyocyte Proliferation Suggests a New Myocardial Regeneration Strategy

Although control and NRG1-treated hearts had the same heart weight 15 weeks after myocardial infarction, NRG1-treated hearts had less hypertrophy at the cardiomyocyte level, as determined by cross-sectional area. This finding suggests that sustained cardiomyocyte replacement may have attenuated the hypertrophic drive after myocardial infarction, resulting in improved ventricular remodeling. These results are consistent with improved cardiac function after administration of NRG1 in a variety of animal models of heart failure (Liu et al., 2006).

Collectively, we have identified the major elements of a new approach to promote myocardial regeneration. These elements include identification of an exogenous activator (NRG1) of proliferation of differentiated cardiomyocytes; the receptor mechanism (ErbB4) that, when activated, initiates cardiomyocyte proliferation; the type of cells (mononucleated) that respond to activation; and the percentage of these cells that respond. Many efforts and important advances have been made toward the goal of developing stem-cell based strategies to regenerate damaged tissues in the heart as well as in other organs. The work presented here suggests that stimulating differentiated cardiomyocytes to proliferate may be a viable alternative that could be developed into a simple strategy to promote myocardial regeneration in mammals.

EXPERIMENTAL PROCEDURES

Cell-Cycle Activity In Vitro

Experiments were approved by the Animal Care and Use Committee. Ventricular cardiomyocytes were isolated from male Wistar rats (12 weeks old, 300 g, Charles River Laboratories; Engel et al., 2005). We added NRG1 (EGF-like domain, amino acids 176–246; 100 ng/ml, R&D Systems), the peptide consisting of the four fasciclin 1 domains of human periostin (500 ng/ml; BioVendor), FGF1 (100 ng/ml; R&D Systems), HB-EGF (10 ng/ml; R&D Systems), or

PDGF-BB (10 ng/ml; Peprotech). For detection of DNA synthesis, we added BrdU (30 μM) for the last three days. The c-ErbB2/Neu blocking antibody was from Calbiochem.

Mouse Strains, Cardiomyocyte Proliferation, and Genetic Fate Tracking In Vivo

We provide a detailed description of mouse strains in the Supplemental Experimental Procedures. We used the α-*MHC-MerCreMer* strain (Sohal et al., 2001) to delete the loxP-flanked exon 2 of *ErbB4* (Golub et al., 2004). We injected tamoxifen in mice with two alleles of α-*MHC-MerCreMer* and one (control) or two (test) *ErbB4* alleles with floxed exon 2. Recombination was detected in 83.5% ± 2% of cardiomyocytes (n = 7; Figure S2C). We used heterozygotes of the α-*MHC-ErbB4* transgenic strain to increase ErbB4 expression (Tidcombe et al., 2003). NRG1 (2.5 μg/mouse dissolved in 0.1% bovine serum albumin, i.p.) or 0.1% bovine serum albumin were injected daily for 9 days. To determine the efficiency of recombination, for genetic fate tracking experiments, to analyze clonal proliferation of cardiomyocytes, and to determine the contribution of stem cells, we crossed the α-*MHC-MerCreMer* allele into the *Rosa26lacZ* strain (Soriano, 1999), injected tamoxifen, and analyzed β-galactosidase-positive and -negative cardiomyocytes. Injections of BrdU (70 μmol/kg, i.p.), with a tissue half-life of 2 hr, were given every 12 hr. For continuous labeling, one injection of thymidine analog was given followed by addition to the drinking water (1 mg/ml) for 9 days (Teta et al., 2007). Cardiomyocytes were isolated 24 hr later by Langendorff perfusion with collagenase II (20 mg/ml, Invitrogen) and protease XIV (5 mg/ml, Sigma). Cell-cycle activity and number of cardiomyocyte nuclei were determined by immunofluorescence microscopy.

Microscopy, Cardiomyocyte Volumes and Cross-Sectional Area, and Sarcomere Disassembly

Immunofluorescence microscopy and fate tracking in vitro were performed as described elsewhere (Kuhn et al., 2007). We used primary antibodies against tropomyosin (Developmental Studies Hybridoma Bank), troponin I (Santa Cruz), BrdU (Abcam), and aurora B kinase (BD Biosciences) for detection and Alexa-fluorophore-conjugated secondary antibodies (Invitrogen) for visualization. We visualized nuclei with 4′,6′-diamidino-phenylindole (DAPI, Invitrogen). The γ value for image acquisition was set at one. Lookup table settings were linear (details of image acquisition in Table S7). For live cell imaging, we maintained cardiomyocytes in an environmental chamber (Tokai-HIT) fitted on the motorized stage (Prior) of an inverted Olympus IX-81 microscope. We used adenoviral transduction to express a fusion construct of histone 2B-GFP under control of the chicken troponin T promoter (cTNT-H2B-GFP; Kuhn et al., 2007). Movies were acquired with a 20× objective, NA 0.45, by a CCD (Hamamatsu) at multiple locations in 1-hr intervals. To determine cardiomyocyte dimensions and volume, we visualized cardiac contractile apparati in isolated cardiomyocytes with an antibody against troponin I (Santa Cruz Biotechnology), acquired confocal stacks with a step size of 0.5 μm, and analyzed by histomorphometry. To determine cardiomyocyte cross-sectional area, we stained cryosections of 14 μm thickness with Masson's Trichrome and determined the area after digital thresholding (Metamorph, Molecular Devices). To determine sarcomere disassembly, we stained cryosections with either α-actinin (Sigma) or myomesin (Developmental Studies Hybridoma Bank) antibodies to visualize Z-disk or M-band, respectively. Karyokinesis was visualized with a phosphorylated histone H3 antibody (Upstate). Cytokinesis was visualized with an antibody against aurora B kinase (Sigma). Images were obtained using a spinning-disk confocal microscope (DSU, Olympus).

Determination of Cardiomyocyte and Stem Cell Contribution

We provide a detailed description of these methods in Supplemental Experimental Procedures. Briefly, to visualize proliferation of individual cardiomyocytes in vivo, we induced sparse genetic labeling in α-*MHC-MerCreMer*$^{+/+}$; *Rosa26R*$^{+/-}$ mice with tamoxifen (5 μg/gm i.p. × 1), injected NRG1, and quantified clusters of one, two, and more genetically labeled cardiomyocytes on X-gal-stained sections. To determine the contribution of undifferentiated stem and progenitor cells, we genetically labeled differentiated cardiomyocytes in α-*MHC-MerCreMer*$^{+/+}$; *Rosa26R*$^{+/-}$ mice. If NRG1-induced cardiomyocyte cell-cycle activity originated from differentiated cardiomyocytes, the proliferative rate should be identical in genetically labeled and unlabeled cardiomyocytes, irrespective of the percentage of genetically labeled cardiomyocytes. In contrast, if the NRG1-induced cardiomyocyte cell-cycle activity originated from undifferentiated progenitor cells, the proliferative rate should change with the percentage of genetically labeled cardiomyocytes. We addressed these possibilities by quantifying the proliferative rate of X-gal-positive and -negative cardiomyocytes across a range of labeling efficiencies.

Quantification of Myocardial Function and Regeneration

We performed sedated echocardiography using a VisualSonics device with a 40 MHz probe. To quantify myocardial regeneration, we analyzed 1.5× magnification pictures of AFOG-stained cryosections (Kuhn et al., 2007). Cardiomyocyte nuclei were counted using the optical dissector method. Cardiomyocyte apoptosis was determined using the ApopTag Red In Situ apoptosis detection kit (Chemicon).

Statistical Analyses

Investigators (K.B., S.A., B.H., and B.K.) quantified observations independently from one another and in a blinded manner (details in Table S8). Numeric data are presented as mean ± standard error of the mean (SEM). We tested statistical significance with the *t*-test and analysis of variance (ANOVA). We used sigmoidal nonlinear or linear regression to fit data (GraphPad). The α-value was set at 0.05.

SUPPLEMENTAL DATA

Supplemental Data include Supplemental Experimental Procedures, seven figures, eight tables, and two movies and can be found with this article online at http://www.cell.com/supplemental/S0092-8674(09)00522-4.

ACKNOWLEDGMENTS

We acknowledge the Mutant Mouse Repository (UC Davis) for providing *ErbB4*$^{F/F}$ mice and Jackson Laboratories for providing α-*MHC-MerCreMer* and *Rosa26R* mice. We thank V. Bezzerides, R. Breitbart, D. Clapham, G. Corfas, C. Hug, and R. Liao (Harvard Medical School), R. Hajjar (Mount Sinai School of Medicine), and E. Oancea (Brown University) for stimulating discussions and E. Long (Children's Hospital) and S. Ngoy (Brigham and Women's Hospital) for technical assistance. This research was supported by the Department of Cardiology at Children's Hospital Boston, the Charles Hood Foundation, and the American Heart Association. B.K. is a founder of CardioHeal.

Received: August 18, 2008
Revised: December 2, 2008
Accepted: April 28, 2009
Published: July 23, 2009

REFERENCES

Ahuja, P., Sdek, P., and MacLellan, W.R. (2007). Cardiac myocyte cell cycle control in development, disease, and regeneration. Physiol. Rev. *87*, 521–544.

Bergmann, O., Bhardwaj, R.D., Bernard, S., Zdunek, S., Barnabe-Heider, F., Walsh, S., Zupicich, J., Alkass, K., Buchholz, B.A., Druid, H., et al. (2009). Evidence for cardiomyocyte renewal in humans. Science *324*, 98–102.

Bettencourt-Dias, M., Mittnacht, S., and Brockes, J.P. (2003). Heterogeneous proliferative potential in regenerative adult newt cardiomyocytes. J. Cell Sci. *116*, 4001–4009.

Chaudhry, H.W., Dashoush, N.H., Tang, H., Zhang, L., Wang, X., Wu, E.X., and Wolgemuth, D.J. (2004). Cyclin A2 mediates cardiomyocyte mitosis in the postmitotic myocardium. J. Biol. Chem. *279*, 35858–35866.

Chen, X., Wilson, R.M., Kubo, H., Berretta, R.M., Harris, D.M., Zhang, X., Jaleel, N., MacDonnell, S.M., Bearzi, C., Tillmanns, J., et al. (2007). Adolescent feline heart contains a population of small, proliferative ventricular myocytes with immature physiological properties. Circ. Res. *100*, 536–544.

Dor, Y., Brown, J., Martinez, O.I., and Melton, D.A. (2004). Adult pancreatic beta-cells are formed by self-duplication rather than stem-cell differentiation. Nature *429*, 41–46.

Engel, F.B., Hsieh, P.C., Lee, R.T., and Keating, M.T. (2006). FGF1/p38 MAP kinase inhibitor therapy induces cardiomyocyte mitosis, reduces scarring, and rescues function after myocardial infarction. Proc. Natl. Acad. Sci. USA *103*, 15546–15551.

Engel, F.B., Schebesta, M., Duong, M.T., Lu, G., Ren, S., Madwed, J.B., Jiang, H., Wang, Y., and Keating, M.T. (2005). p38 MAP kinase inhibition enables proliferation of adult mammalian cardiomyocytes. Genes Dev. *19*, 1175–1187.

Fazel, S., Cimini, M., Chen, L., Li, S., Angoulvant, D., Fedak, P., Verma, S., Weisel, R.D., Keating, A., and Li, R.K. (2006). Cardioprotective c-kit+ cells are from the bone marrow and regulate the myocardial balance of angiogenic cytokines. J. Clin. Invest. *116*, 1865–1877.

Fuller, S.J., Sivarajah, K., and Sugden, P.H. (2008). ErbB receptors, their ligands, and the consequences of their activation and inhibition in the myocardium. J. Mol. Cell. Cardiol. *44*, 831–854.

Gassmann, M., Casagranda, F., Orioli, D., Simon, H., Lai, C., Klein, R., and Lemke, G. (1995). Aberrant neural and cardiac development in mice lacking the ErbB4 neuregulin receptor. Nature *378*, 390–394.

Golub, M.S., Germann, S.L., and Lloyd, K.C. (2004). Behavioral characteristics of a nervous system-specific erbB4 knock-out mouse. Behav. Brain Res. *153*, 159–170.

Guha, A., Lin, L., and Kornberg, T.B. (2008). Organ renewal and cell divisions by differentiated cells in *Drosophila*. Proc. Natl. Acad. Sci. USA *105*, 10832–10836.

Hsieh, P.C., Segers, V.F., Davis, M.E., Macgillivray, C., Gannon, J., Molkentin, J.D., Robbins, J., and Lee, R.T. (2007). Evidence from a genetic fate-mapping study that stem cells refresh adult mammalian cardiomyocytes after injury. Nat. Med. *13*, 970–974.

Katz, E.B., Steinhelper, M.E., Delcarpio, J.B., Daud, A.I., Claycomb, W.C., and Field, L.J. (1992). Cardiomyocyte proliferation in mice expressing alpha-cardiac myosin heavy chain-SV40 T-antigen transgenes. Am. J. Physiol. *262*, H1867–H1876.

Keefe, D.L. (2002). Trastuzumab-associated cardiotoxicity. Cancer *95*, 1592–1600.

Kuhn, B., Del Monte, F., Hajjar, R.J., Chang, Y.S., Lebeche, D., Arab, S., and Keating, M.T. (2007). Periostin induces proliferation of differentiated cardiomyocytes and promotes cardiac repair. Nat. Med. *13*, 962–969.

Lee, K.F., Simon, H., Chen, H., Bates, B., Hung, M.C., and Hauser, C. (1995). Requirement for neuregulin receptor erbB2 in neural and cardiac development. Nature *378*, 394–398.

Liu, X., Gu, X., Li, Z., Li, X., Li, H., Chang, J., Chen, P., Jin, J., Xi, B., Chen, D., et al. (2006). Neuregulin-1/erbB-activation improves cardiac function and survival in models of ischemic, dilated, and viral cardiomyopathy. J. Am. Coll. Cardiol. *48*, 1438–1447.

Meyer, D., and Birchmeier, C. (1995). Multiple essential functions of neuregulin in development. Nature *378*, 386–390.

Pasumarthi, K.B., and Field, L.J. (2002). Cardiomyocyte cell cycle regulation. Circ. Res. *90*, 1044–1054.

Pasumarthi, K.B., Nakajima, H., Nakajima, H.O., Soonpaa, M.H., and Field, L.J. (2005). Targeted expression of cyclin D2 results in cardiomyocyte DNA synthesis and infarct regression in transgenic mice. Circ. Res. *96*, 110–118.

Poss, K.D., Wilson, L.G., and Keating, M.T. (2002). Heart regeneration in zebrafish. Science *298*, 2188–2190.

Rawlins, E.L., and Hogan, B.L. (2006). Epithelial stem cells of the lung: privileged few or opportunities for many? Development *133*, 2455–2465.

Sena, G., Wang, X., Liu, H.Y., Hofhuis, H., and Birnbaum, K.D. (2009). Organ regeneration does not require a functional stem cell niche in plants. Nature *457*, 1150–1153.

Sohal, D.S., Nghiem, M., Crackower, M.A., Witt, S.A., Kimball, T.R., Tymitz, K.M., Penninger, J.M., and Molkentin, J.D. (2001). Temporally regulated and tissue-specific gene manipulations in the adult and embryonic heart using a tamoxifen-inducible Cre protein. Circ. Res. *89*, 20–25.

Soonpaa, M.H., and Field, L.J. (1998). Survey of studies examining mammalian cardiomyocyte DNA synthesis. Circ. Res. *83*, 15–26.

Soriano, P. (1999). Generalized lacZ expression with the ROSA26 Cre reporter strain. Nat. Genet. *21*, 70–71.

Tatsuka, M., Katayama, H., Ota, T., Tanaka, T., Odashima, S., Suzuki, F., and Terada, Y. (1998). Multinuclearity and increased ploidy caused by overexpression of the aurora- and Ipl1-like midbody-associated protein mitotic kinase in human cancer cells. Cancer Res. *58*, 4811–4816.

Teta, M., Rankin, M.M., Long, S.Y., Stein, G.M., and Kushner, J.A. (2007). Growth and regeneration of adult beta cells does not involve specialized progenitors. Dev. Cell *12*, 817–826.

Tidcombe, H., Jackson-Fisher, A., Mathers, K., Stern, D.F., Gassmann, M., and Golding, J.P. (2003). Neural and mammary gland defects in ErbB4 knockout mice genetically rescued from embryonic lethality. Proc. Natl. Acad. Sci. USA *100*, 8281–8286.

Wang, Z., Xu, G., Wu, Y., Guan, Y., Cui, L., Lei, X., Zhang, J., Mou, L., Sun, B., and Dai, Q. (2008). Neuregulin-1 enhances differentiation of cardiomyocytes from embryonic stem cells. Med. Biol. Eng. Comput. *47*, 41–48.

Weaver, M., and Krasnow, M.A. (2008). Dual origin of tissue-specific progenitor cells in *Drosophila* tracheal remodeling. Science *321*, 1496–1499.

Wills, A.A., Holdway, J.E., Major, R.J., and Poss, K.D. (2008). Regulated addition of new myocardial and epicardial cells fosters homeostatic cardiac growth and maintenance in adult zebrafish. Development *135*, 183–192.